Persistent Ballistic Entanglement Spreading with Optimal Control in Quantum Spin Chains

Ying Lu, Pei Shi, Xiao-Han Wang, Jie Hu, and Shi-Ju Ran[*]

Center for Quantum Physics and Intelligent Sciences, Department of Physics, Capital Normal University, Beijing 10048, China

Entanglement propagation provides a key routine to understand quantum many-body dynamics in and out of equilibrium. Entanglement entropy (EE) usually approaches to a subsaturation known as the Page value $\tilde{S}_P = \tilde{S} - dS$ (with $\tilde{S}$ the maximum of EE and dS the Page correction) in, e.g., the random unitary evolutions. The ballistic spreading of EE usually appears in the early time and will be deviated far before the Page value is reached. In this work, we uncover that the magnetic field that maximizes the EE robustly induces persistent ballistic spreading of entanglement in quantum spin chains. The linear growth of EE is demonstrated to persist until the maximal $\tilde{S}$ (along with a flat entanglement spectrum) is reached. The robustness of ballistic spreading and the enhancement of EE under such an optimal control are demonstrated, considering particularly perturbing the initial state by random pure states (RPSs). These are argued as the results from the endomorphism of the time evolution under such an entanglement-enhancing optimal control for the RPSs.

Quantum entanglement is a fundamental concept to reveal the essence of quantum systems in contrast to classical ones [1,2]. The dynamics of quantum entanglement under unitary time evolution provides a key routine to investigating the exotic phenomena and properties of quantum many-body physics, such as quasiparticle excitations [3,4], information propagation [5–8], many-body localization [9–16], and causality [17].

Among the novel phenomena in quantum many-body dynamics, the emergence of ballistic transport of entanglement attracts much attention. It is mostly observed in the integrable models, indicating the presence of quasiparticle propagations [3,18,19]. Exceptions have been found where ballistic spreading appears in the diffusive nonintegrable systems [20–22]. In both cases, the bipartite entanglement entropy (EE) grows linearly with time according to the Kardar-Parisi-Zhang equation [23,24]. Other examples exhibiting this property include the random unitary dynamics [25,26] and Floquet spin models [27].

However, previous works suggest that the ballistic spreading persists generally in a relatively short time, and the EE eventually converges to a subsaturation known as the Page value [28]

$$\tilde{S}_P = \tilde{S} - \frac{N_A}{2\ln 2 N_B} - O\left(\frac{1}{2^N}\right), \qquad (1)$$

where $\tilde{S} = \log_2 2^{N_A} = N_A$ is the maximum of EE, N is the total number of spins, N_A and N_B are the numbers of spins

in the two subsystems, respectively (with $N_A + N_B = N$; we take $N_A = N_B$ below for simplicity), and $O(1/2^N)$ represents the rest of the higher-order contributions. Equation (1) can be deduced from the random matrix theory. The final state is similar to a random pure state (RPS) [20,28]. It is thus of theoretical and practical interest to seek the dynamical processes where the EE exceeds the Page value with persistent ballistic spreading behavior during the evolution.

In this work, we show that quantum control by magnetic field can robustly reach the maximal $\tilde{S}$. Different EEs reachable by some typical 1D quantum systems are illustrated in Fig. 1. The magnetic field is determined variationally by maximizing the EE in the center of the final state, which is dubbed the "variational entanglement-enhancing" field (VEEF). Different from the previous works [29,30], ballistic spreading of entanglement is observed, where the EE $S(t)$ at the time t obeys

$$S(t) \simeq vt, \qquad (2)$$

with v the velocity. The linear growth with VEEF will persist till the EE reaches $\tilde{S} = N/2$, when the evolution time T satisfies

$$T \leq T_S \equiv \frac{N}{2v}. \qquad (3)$$

Note T_S can be defined when the linear growth of EE can persist until $\tilde{S}$ is reached. In this case, the velocity defined as $v = dS(t)/dt$ is a constant for $t \leq T_S$. For $T > T_S$, the EE still increases to the maximum $\tilde{S}$ at $t = T$. But during
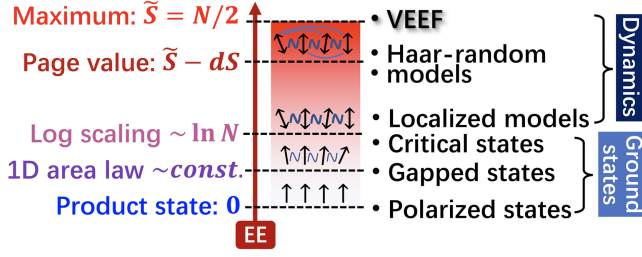
FIG. 1. The illustration of different EEs (with equal bipartition) reachable by the 1D quantum systems with some typical examples listed in the right-hand side. The wavy lines among the arrows indicate the strength of entanglement.

the evolution, the instantaneous velocity $v(t) \equiv dS(t)/dt$ is allowed to vary [in fact, one has $v(t) \leq v = \tilde{S}/T_S$, where v can be considered as the maximal velocity that the system can reach]. In the case of $T = T_S$ in comparison, the instantaneous velocity $v(t)$ has to be constantly v so that the EE can reach $\tilde{S} = vT_S$ at $t = T$. We also demonstrate the persistent ballistic spreading of EE on a localized model with VEEF. Generally, EE should spread subballistically in the localized models [9,10,31].

The persistent ballistic spreading of EE is shown to be robust under random perturbations. A collapsing point is given by the EE curves from the initial states perturbed by different strengths of randomness. Such a behavior is explained and analyzed based on the random unitary evolution and the endomorphism of the VEEF evolution for the RPSs.

Variational entanglement-enhancing field—Recent works revealed the inspiring prospective on applying machine learning (ML) methods in studying quantum dynamics and control [32–41]. Here, our aim is to enhance quantum entanglement by developing a ML-assisted quantum-control scheme. Enhancing entanglement [29,30,42,43] is important since entanglement is a fragile resource in noisy environments.

We consider the time evolution with the Hamiltonian

$$\hat{H}(t) = \sum_{m,n} \hat{H}_{mn} + \sum_n \sum_{\alpha=x,z} h_n^\alpha(t)\hat{\sigma}_n^\alpha, \quad (4)$$

where $\hat{H}_{mn}$ represents the time-independent two-body interaction between the mth and nth sites, $\hat{\sigma}_n^\alpha$ is the Pauli operator ($\alpha = $ x, y, z) on the nth site, and $h_n^\alpha(t)$ denotes the time-dependent field. The time evolution is a mapping

$$\mathcal{U}: |\psi_0\rangle \to |\psi(t)\rangle = e^{-i\int_{\tau=0}^t \hat{H}(\tau)d\tau}|\psi_0\rangle, \quad (5)$$

with $|\psi_0\rangle$ the initial state. Here, we consider $h_n^\alpha(t)$ as the variational parameters of $\mathcal{U}$, and optimize them by maximizing the EE S of the final state $|\psi(T)\rangle$ (with T the total evolution time). We dub the field satisfying the maximization condition $\partial S(T)/\partial h_n^\alpha(t) = 0$ as the

variational entanglement-enhancing field. In other words, the "VEEF dynamics" shows the properties of $\mathcal{U}$ by imposing $\partial S(T)/\partial h_n^\alpha(t) = 0$.

To obtain VEEF, we adopt the automatic differentiation technique that originated from the field of ML [40,44]. The time evolution is simulated by means of Trotter-Suzuki decomposition [45,46]. In the simulations, we take the Planck constant $\hbar = 1$ as the energy scale, and the time discretization for $h_n^\alpha(t)$ as $\tau = 1/64 \sim O(10^{-2})$ (which determines the highest frequency of $h_n^\alpha(t)$). With the bipartition to two halves denoted as A and B, the EE of $|\psi(t)\rangle$ satisfies

$$S(t) = -\text{Tr}_A[\hat{\rho}(t)\log_2\hat{\rho}(t)], \quad (6)$$

with $\hat{\rho}(t) = \text{Tr}_B|\psi(t)\rangle\langle\psi(t)|$ the reduced density matrix of A by tracing over the degrees of freedom of B. The same results will be obtained by the reduced density matrix of B. The maximal point is reached by using the gradient descent method, $h_n^\alpha(t)$ as $h_n^\alpha(t) \leftarrow h_n^\alpha(t) + \eta[\partial S(T)/\partial h_n^\alpha(t)]$ with $S(T)$ the EE measured at the center of the final state. The gradients are obtained by the automatic differentiation technique and η is the gradient step (or the learning rate in term of ML). To enhance the stability, we employ the fine-grained time optimization strategy [40], and the ADAM optimizer [47] that has been widely used in ML.

Without losing generality, we take the initial state as a product state $|\psi_0\rangle = \prod_{\otimes n=1}^N |s_n\rangle$, where each spin $|s_n\rangle = \cos(\theta_n/2)|0_n\rangle + e^{i\phi_n}\sin(\theta_n/2)|1_n\rangle$ points in a random direction on the Bloch sphere [$\theta_n \in [0, \pi)$ and $\phi_n \in [0, 2\pi)$]. The states $|0_n\rangle$ and $|1_n\rangle$ are the two eigenstates of $\hat{\sigma}_n^z$. Obviously, the initial state is not an eigenstate of the Hamiltonian.

Persistent ballistic spreading of entanglement—We consider the one-dimensional (1D) quantum Ising model (QIM) with periodic boundary condition, whose Hamiltonian can be written as $\hat{H}_{\text{QIM}}(t) = \sum_{n=1}^{N-1} \hat{\sigma}_n^z\hat{\sigma}_{n+1}^z + \hat{\sigma}_1^z\hat{\sigma}_N^z + \sum_{n=1}^N \sum_{\alpha=x,z} h_n^\alpha(t)\hat{\sigma}_n^\alpha$. The field is restricted to the spin x and spin z directions, which is a common scenario in theoretical and experimental investigations [48,49].

Figure 2 demonstrates the $S(t)$ [Eq. (6)] with $N = 10$ spins with the field taken in different ways. The VEEF-driven spreading exhibits persistent linear growth until the maximal EE $\tilde{S}$ is reached (see the purple solid line in Fig. 2 with $T = 1.8 \simeq T_S$). This means $\partial S(T)/\partial h_n^\alpha(t) = 0$ [$\sim O(10^{-8})$ from our numeric results] is satisfied for any $t \leq T_S$, consistent with the persistency of linear EE spreading with VEEF and the fact that 1D chains can at most exhibit linear growth of EE. Note $\tilde{S}$ corresponds to equal Schmidt coefficients ($\Lambda_1 = \Lambda_2 = \cdots$). The matrization of the state coefficients with $S = \tilde{S}$ gives a unitary matrix. Such a state can be regarded as the Choi state of a unitary operator [50]. The measurement on one subsystem of the Choi state will result in a unitary transformation on the collapsed state. In comparison, the Schmidt coefficients of
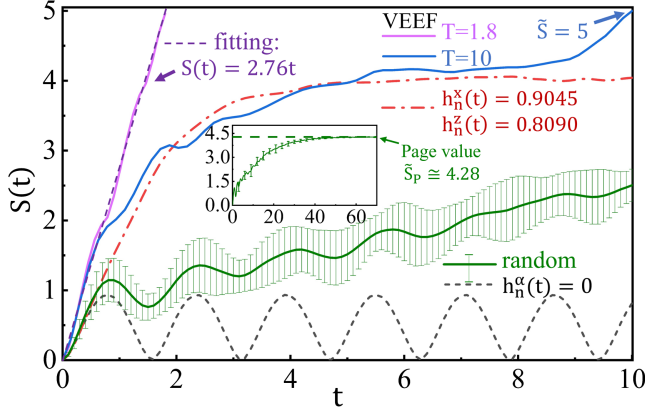
FIG. 2. The EE $S(t)$ against time t with zero field $h_n^\alpha(t) = 0$ (black dashed line), the constant field $h_n^x(t) = 0.9045$ and $h_n^z(t) = 0.8090$ where the system is nonintegrable [20] (red dash-dot line), random $h_n^\alpha(t)$ (green solid line), and VEEF ($T = 1.8$ by purple solid line and $T = 10$ by blue solid line). We here consider the $N = 10$ quantum Ising chain with periodic boundary condition. The inset shows that EE converges to the Page value [Eq. (1)] in the long-time limit [28]. The results with the random $h_n^\alpha(t)$ are estimated by implementing ten independent simulations, where the variance is indicated by the error bars.

the states whose EEs give the Page value deviate from being equal, particularly for moderately large sizes [51,61]. We have $T_S = 1.81$ by Eq. (3) for the 1D QIM. The velocity $v = 2.76$ with VEEF is much larger than $v = 1.65$ obtained with the fixed field $h_n^x(t) = 0.9045$, $h_n^z(t) = 0.8090$ (where the system robustly becomes nonintegral [20,27,62–67]). The linear growth of $S(t)$ is only observed at the early time (for about $t < 3$) with such a fixed field.

For $h_n^\alpha(t) = 0$, all terms in the Hamiltonian commute with each other and $S(t)$ oscillates with t far below the Page value [27]. With random $h_n^\alpha(t)$, $S(t)$ tends to increase over time, eventually approaching to the Page value in the long-time limit [28] (about $t > 60$ shown in the inset), behaving on average like a random pure state [20]. In short, the previous means of implementing field reach the Page value of EE and induce a linear growth at the early time with a lower velocity.

Extra degrees of freedom emerges for the paths to a state with a maximal EE $\tilde{S}$ for $T > T_S$. A consequence is that the linear growth is deviated before $\tilde{S}$ is achieved (see the blue solid line in Fig. 2 with $T = 10 \gg T_S$), meaning $\partial S(T)/\partial h_n^\alpha(t) = 0$ may not be satisfied in the duration $t < T$. But $\tilde{S}$ is robustly reached for the final state.

Figure 3 demonstrates the ability of VEEF on changing the behaviors of EE spreading (that reflects the information spreading) from being diffusive to ballistic. The diffusive spreading of EE usually appears in the localized models [9,10,31]. We take the XXZ chain with periodic boundary condition, where the local interaction satisfies $\hat{H}_{n,n+1} = \hat{\sigma}_n^x \hat{\sigma}_{n+1}^x + \hat{\sigma}_n^y \hat{\sigma}_{n+1}^y + \delta \hat{\sigma}_n^z \hat{\sigma}_{n+1}^z$ (with $\delta = 3$ in Fig. 3) and the VEEF is restricted in the x and z directions. With the zero or
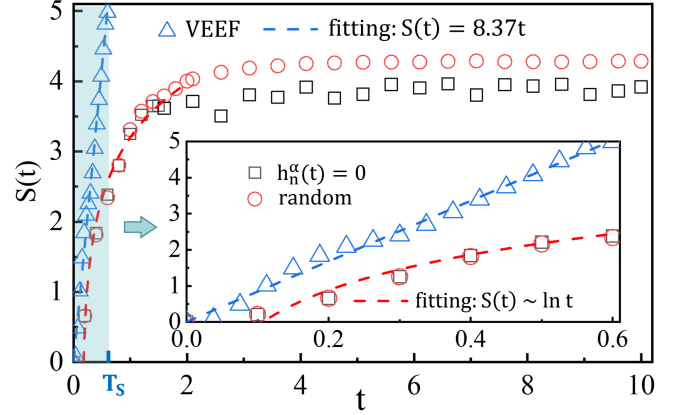

FIG. 3. The EE $S(t)$ for the $N = 10$ XXZ model obeys the logarithmic (diffusive) spreading with zero or random field [9,10], but the linear (ballistic) spreading with VEEF. The inset shows the enlargement of the area for $t \leq T_S$.

random field, diffusive spreading is expected, with $S(t) \sim \ln t$ [9,10]. With VEEF, linear growth $S(t) \sim vt$ with $v \simeq 8.37$ is obtained, which persists till $\tilde{S}$ is reached at $t = T_s$.

Robustness—Figure 4 demonstrates the robustness of the ballistic EE spreading for different total evolution times T. The inset shows that the curves with different T's "perfectly" collapse to the linear relation given by Eq. (2) for the early times. In all cases, $\tilde{S}$ is reached for the final state. Note the states with the maximal EE are obviously not unique but form a subspace. The coefficients of a state therein is a unitary matrix from its Schmidt decomposition $\Psi = UV^\dagger/Z$ (with Z denotes the normalization factor), where the Schmidt coefficients are equal.

We conjecture that the whole subspace with maximal EE is in principle accessible by the VEEF for any $T \geq T_S$. To verify this conjecture, we take the target state as $|\psi(T')\rangle$ with $T' \geq T_S$ and its EE $S = \tilde{S}$, and try to evolve a random product state to $|\psi(T')\rangle$ in an evolution time $T > T_S$. The
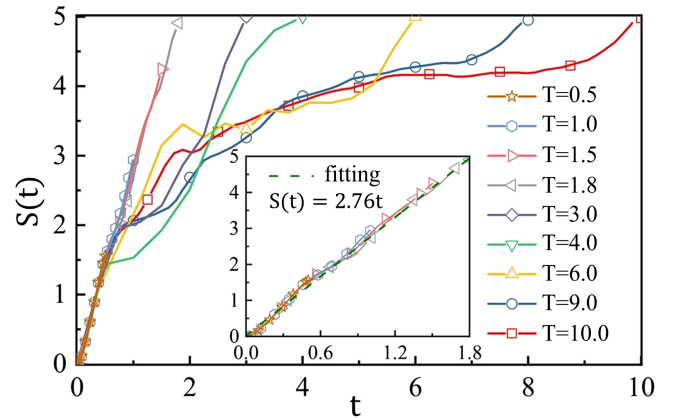

FIG. 4. The EE $S(t)$ of the 1D QIM ($N = 10$) against the time t with different total evolution time T. The inset shows the $S(t)$ for $T < T_S$, which satisfies the linear relation $S(t) = 2.76t$.
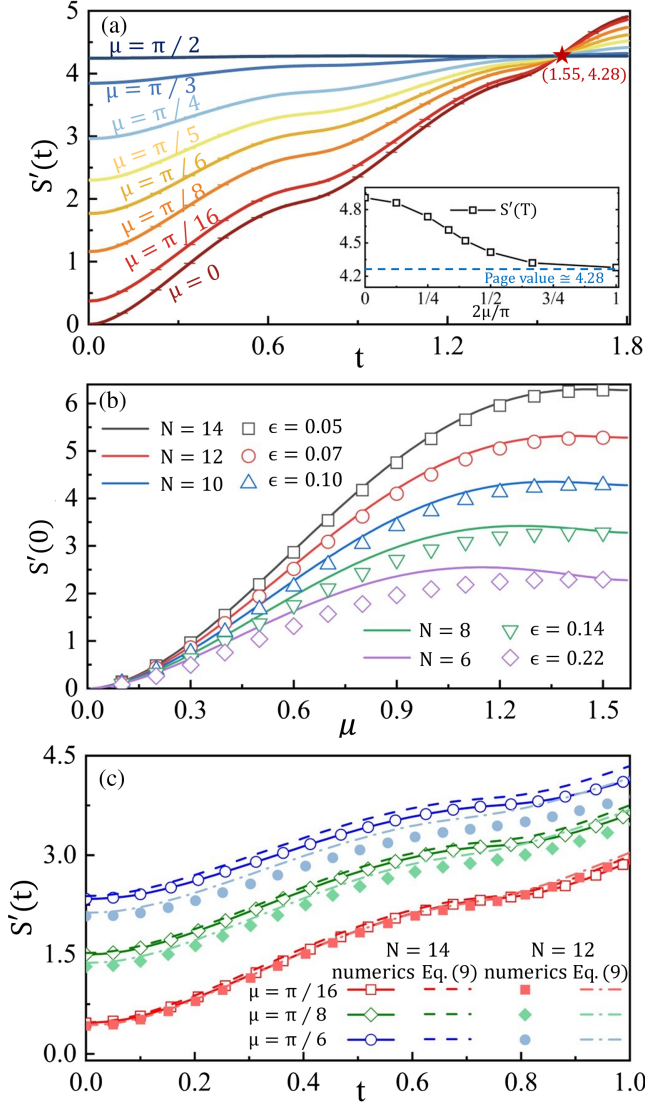
FIG. 5. (a) The EE $S'(t)$ of 1D QIM against time t for the initial states $|\psi'_0\rangle$ with different μ controlling the strength of random perturbation [Eq. (7)]. $|\psi_0\rangle$ is the unperturbed initial state for obtaining the VEEF, and $|\psi_r\rangle$ is a RPS. The results are the average of 10 independent simulations, and the error bars ($\sim O(10^{-3})$) are given by the variances. The insets show the $S'(T)$ versus μ. (b) The EE $S'(0)$ of the perturbed initial state vs μ for different system sizes N, obtained by numerical simulations (symbols) and by Eq. (9) (solid lines). The violation of the orthogonal conditions is characterized by ϵ. (c) The $S'(t)$ obtained by numerical simulations (symbols) and by Eq. (9) (solid lines) for $N = 12, 14$ and $\mu = \pi/6, \pi/8, \pi/16$.

field is optimized by minimizing the infidelity $F_{\text{in}}(T; T') = 1 - |\langle\psi(T')|e^{-i\int_{\tau=0}^{t}\hat{H}(\tau)d\tau}|\psi(0)\rangle|$ [40]. Taking $T = 4$, $T' = 6$ ($T < T'$) and $T = 6$, $T' = 4$ ($T > T'$) as two examples, vanishing infidelity with $F_{\text{in}}(T; T') \sim O(10^{-4})$ is obtained, which supports our conjecture.

From the optimization process, VEEF should depend on the choice of the initial state $|\psi_0\rangle$. Figure 5 illustrates the robustness against random perturbations on $|\psi_0\rangle$ by

$$|\psi'_0\rangle = \cos\mu|\psi_0\rangle + \sin\mu|\psi_r\rangle, \qquad (7)$$

with μ controlling the strength of perturbation and $|\psi_r\rangle$ a RPS whose coefficients are randomly generated with a normal distribution. For $\mu = 0$, no perturbation is added and the EE $S'(t)$ satisfies Eq. (2). For $\mu = \pi/2$, the evolution starts from a RPS with $S'(t = 0) \simeq \tilde{S}_P$, and $S'(t)$ is almost a constant. This shows the time evolution $\mathcal{U}$ with VEEF is "endomorphic" for the RPS subspace, i.e., $\mathcal{U}_{\text{VEEF}}(|\psi_r\rangle) \in \text{RPS}$ for $|\psi_r\rangle \in \text{RPS}$. The VEEF evolution (optimized with a specific initial state) resembles the random unitary evolution when taking a RPS as the initial state.

For an arbitrary μ, the perturbed initial state is the weighted superposition between the original initial state and a RPS. The perturbation preserves the linear behavior of EE but with lower velocities. This is reasonable since adjusting the field (one-body operators) does not alter the structure of the underlying quantum circuit, and therefore essentially does not change the Haar dynamics for the evolution of the RPS part (recall the endomorphism of $\mathcal{U}$ with VEEF, which maps a RPS to RPS). The data collapse at the crossing point of the two curves $S'(t) = vt$ [Eq. (2) with no perturbation] and $S'(t) = \tilde{S}_P$ (Page value with RPS). Consequently, we have $S'(T) \rightarrow \tilde{S}_P$ as $\mu \rightarrow (\pi/2)$ [see the inset of Fig. 5(a)]. This implies we could exceed the Page value $S'(T) > \tilde{S}_P$ by implementing VEEF on an initial state $|\psi'_0\rangle$ with $|\langle\psi_0|\psi'_0\rangle| > 0$ when the orthogonal part is described by a RPS. In this case, the perturbation will enlarge the EE [$S'(t) > S(t)$ with $S(t)$ the EE without perturbation] for the time duration before the collapsing point.

To further analyze $S'(t)$, we assuming the following orthogonal conditions between the Schmidt basis states of $|\psi_0\rangle$ and $|\psi_r\rangle$ as

$$_i\langle\psi^A(t)|\psi_r^A(t)\rangle_{i'} \sim 0, \qquad _i\langle\psi^B(t)|\psi_r^B(t)\rangle_{i'} \sim 0. \quad (8)$$

with $\{|\psi^A(t)\rangle_i, |\psi^B(t)\rangle_i\}$ and $\{|\psi_r^A(t)\rangle_i, |\psi_r^B(t)\rangle_i\}$ the left or right Schmidt basis states of $\mathcal{U}_{\text{VEEF}}(|\psi_0\rangle)$ and $\mathcal{U}_{\text{VEEF}}(|\psi_r\rangle)$, respectively. Then, the EE approximately obeys

$$S'(t) \simeq \tilde{S}_\mu + \tilde{S}_P\sin^2\mu + S(t)\cos^2\mu, \qquad (9)$$

where $\tilde{S}_\mu = -\cos^2\mu\log_2\cos^2\mu - \sin^2\mu\log_2\sin^2\mu$ can be treated as an additional entropy from a two-level probabilistic distribution $p(\mu) = [\cos^2\mu, \sin^2\mu]$ [51]. Equation (9) implies the linear growth of $S'(t)$ since $S(t)$ satisfies Eq. (2).

At $t = 0$, the EE of the initial state can be well predicted by Eq. (9), particularly for $N = 14$, since the orthogonal conditions between a RPS and a product state can be well satisfied with a moderately large N [see Fig. 5(b); note $S(0) = 0$]. The violation of Eq. (8) is

characterized by $\epsilon = (1/2D)\left(\sum_{i=1}^{D}\left|\langle\psi^{A}(0)|\psi_{r}^{A}(0)\rangle_{i}\right| + \sum_{i=1}^{D}\left|\langle\psi^{B}(0)|\psi_{r}^{B}(0)\rangle_{i}\right|\right)$, which should, in general, vanish exponentially in the $N \to \infty$ limit. For $t > 0$, the deviation between the VEEF results and Eq. (9) is small for small μ and t, and for large N [Fig. 5(c)]. For large μ or t, we essentially require the corresponding orthogonality between a RPS and an entangled state, which is more difficult to achieve and thus requires larger N [51]. We expect Eq. (9) to be held for $N \to \infty$.

Summary—We have uncovered the persistent ballistic spreading of entanglement under the variational entanglement-enhancing field that maximizes the entanglement entropy of the final state. By persistent, we mean that the linear growth of EE (with equal bipartition) holds until the maximal EE is reached. This is in contrast to the previous results, where the EE generally converges to the Page value in the long-time limit and the linear growth just appears at the early time of evolution. The robustness of the EE ballistic spreading under VEEF is investigated. When the perturbation is described by a random pure state (RPS), the VEEF can enlarge the EE in a predictable manner and its persistent linear growth can be preserved. This is a result of the endomorphism of the VEEF time evolution for the RPSs.

[1] J. S. Bell and A. Aspect, *Speakable and Unspeakable in Quantum Mechanics: Collected Papers on Quantum Philosophy*, 2nd ed. (Cambridge University Press, Cambridge, England, 2004), 10.1017/CBO9780511815676.

[2] M. A. Nielsen and I. L. Chuang, *Quantum Computation and Quantum Information: 10th Anniversary Edition* (Cambridge University Press, Cambridge, England, 2010), 10.1017/CBO9780511976667.

[3] P. Calabrese and J. Cardy, J. Stat. Mech. (2005) P04010.

[4] A. Bastianello and M. Collura, SciPost Phys. **8**, 045 (2020).

[5] P. Jurcevic, B. P. Lanyon, P. Hauke, C. Hempel, P. Zoller, R. Blatt, and C. F. Roos, Nature (London) **511**, 202 (2014).

[6] J. B. Clark, R. T. Glasser, Q. Glorieux, U. Vogl, T. Li, K. M. Jones, and P. D. Lett, Nat. Photonics **8**, 515 (2014).

[7] D. J. Luitz and Y. Bar Lev, Phys. Rev. B **96**, 020406(R) (2017).

[8] W. Zhu, Z. Huang, Y.-C. He, and X. Wen, Phys. Rev. Lett. **124**, 100605 (2020).

[9] M. Žnidarič, T. c. v. Prosen, and P. Prelovšek, Phys. Rev. B **77**, 064426 (2008).

[10] J. H. Bardarson, F. Pollmann, and J. E. Moore, Phys. Rev. Lett. **109**, 017202 (2012).

[11] M. Serbyn, Z. Papić, and D. A. Abanin, Phys. Rev. Lett. **110**, 260601 (2013).

[12] R. Vosk and E. Altman, Phys. Rev. Lett. **110**, 067204 (2013).

[13] D. A. Huse, R. Nandkishore, and V. Oganesyan, Phys. Rev. B **90**, 174202 (2014).

[14] M. Žnidarič, Phys. Rev. B **97**, 214202 (2018).

[15] M. Schulz, C. A. Hooley, R. Moessner, and F. Pollmann, Phys. Rev. Lett. **122**, 040606 (2019).

[16] G. De Tomasi, Phys. Rev. B **99**, 054204 (2019).

[17] J. T. Schneider, J. Despres, S. J. Thomson, L. Tagliacozzo, and L. Sanchez-Palencia, Phys. Rev. Res. **3**, L012022 (2021).

[18] G. D. Chiara, S. Montangero, P. Calabrese, and R. Fazio, J. Stat. Mech. (2006) P03001.

[19] T. Hartman and J. Maldacena, J. High Energy Phys. 05 (2013) 014.

[20] H. Kim and D. A. Huse, Phys. Rev. Lett. **111**, 127205 (2013).

[21] A. Nahum, J. Ruhman, S. Vijay, and J. Haah, Phys. Rev. X **7**, 031016 (2017).

[22] E. Bianchi, L. Hackl, and N. Yokomizo, J. High Energy Phys. 03 (2018) 025.

[23] M. Kardar, G. Parisi, and Y.-C. Zhang, Phys. Rev. Lett. **56**, 889 (1986).

[24] T. Rakovszky, C. W. von Keyserlingk, and F. Pollmann, Phys. Rev. B **100**, 125139 (2019).

[25] K. Zyczkowski and M. Kus, J. Phys. A **27**, 4235 (1994).

[26] M. P. Fisher, V. Khemani, A. Nahum, and S. Vijay, Annu. Rev. Condens. Matter Phys. **14**, 335 (2023).

[27] T. Zhou and D. J. Luitz, Phys. Rev. B **95**, 094206 (2017).

[28] D. N. Page, Phys. Rev. Lett. **71**, 1291 (1993).

[29] K. Hai, W. Hai, and Q. Chen, Phys. Rev. A **82**, 053412 (2010).

[30] Y. Zheng and S.-J. Yang, Eur. Phys. J. Spec. Top. **226**, 2843 (2017).

[31] B. Swingle, arXiv:1307.0507.

[32] P. Palittapongarnpim, P. Wittek, E. Zahedinejad, S. Vedaie, and B. C. Sanders, Neurocomputing;Variable Star Bulletin **268**, 116 (2017).

[33] X.-C. Yang, M.-H. Yung, and X. Wang, Phys. Rev. A **97**, 042324 (2018).

[34] M. Bukov, A. G. R. Day, D. Sels, P. Weinberg, A. Polkovnikov, and P. Mehta, Phys. Rev. X **8**, 031086 (2018).

[35] R.-B. Wu, H. Ding, D. Dong, and X. Wang, Phys. Rev. A **99**, 042327 (2019).

[36] X.-M. Zhang, Z. Wei, R. Asad, X.-C. Yang, and X. Wang, npj Quantum Inf. **5**, 85 (2019).

[37] M. Y. Niu, S. Boixo, V. N. Smelyanskiy, and H. Neven, npj Quantum Inf. **5**, 33 (2019).

[38] F. Schäfer, M. Kloc, C. Bruder, and N. Lörch, Mach. Learn. Sci. Technol. **1**, 035009 (2020).

[39] Y. Zeng, J. Shen, S. Hou, T. Gebremariam, and C. Li, Phys. Lett. A **384**, 126886 (2020).

[40] Y. Lu, Y.-M. Li, P.-F. Zhou, and S.-J. Ran, Phys. Rev. A **104**, 052413 (2021).

[41] T. Huang, Y. Ban, E. Y. Sherman, and X. Chen, Phys. Rev. Appl. **17**, 024040 (2022).

[42] M. Lubasch, F. Mintert, and S. Wimberger, Phys. Rev. A **84**, 063615 (2011).

[43] F. Albarelli, U. Shackerley-Bennett, and A. Serafini, Phys. Rev. A **98**, 062312 (2018).

[44] A. G. Baydin, B. A. Pearlmutter, A. A. Radul, and J. M. Siskind, J. Mach. Learn. Res. **18**, 1 (2018), https://www.jmlr.org/papers/v18/17-468.html.

[45] H. F. Trotter, Proc. Am. Math. Soc. **10**, 545 (1959).

[46] M. Suzuki, Commun. Math. Phys. **51**, 183 (1976).

[47] D. P. Kingma and J. Ba, in *Proceedings of the 3rd International Conference on Learning Representations, ICLR 2015, San Diego, CA, USA, 2015, Conference Track Proceedings* (2015), https://iclr.cc/archive/www/2015.html.

[48] R. Coldea, D. A. Tennant, E. M. Wheeler, E. Wawrzynska, D. Prabhakaran, M. Telling, K. Habicht, P. Smeibidl, and K. Kiefer, Science **327**, 177 (2010).

[49] Y. Y. Atas, E. Bogomolny, O. Giraud, and G. Roux, Phys. Rev. Lett. **110**, 084101 (2013).

[50] D.-S. Wang, Phys. Rev. A **101**, 052311 (2020).

[51] See Supplemental Material at http://link.aps.org/supplemental/10.1103/PhysRevLett.133.070402 for more information on the VEEF, including the enhancement of Rényi entropy, and evolution of Schmidt coefficients, and the robustness against different kinds of random perturbations. Refs. [50,52–61] are included.

[52] P. A. M. Dirac, Math. Proc. Cambridge Philos. Soc. **26**, 376 (1930).

[53] F. Verstraete, J. J. García-Ripoll, and J. I. Cirac, Phys. Rev. Lett. **93**, 207204 (2004).

[54] G. A. L. White, F. A. Pollock, L. C. L. Hollenberg, K. Modi, and C. D. Hill, PRX Quantum **3**, 020344 (2022).

[55] J. Kunjummen, M. C. Tran, D. Carney, and J. M. Taylor, Phys. Rev. A **107**, 042403 (2023).

[56] A. Anshu, A. W. Harrow, and M. Soleimanifar, Nat. Phys. **18**, 1362 (2022).

[57] E. Rico Ortega and S. Montangero, Nat. Phys. **18**, 1278 (2022).

[58] W. W. Ho and D. A. Abanin, Phys. Rev. B **95**, 094302 (2017).

[59] T. Rakovszky, F. Pollmann, and C. W. von Keyserlingk, Phys. Rev. Lett. **122**, 250602 (2019).

[60] Y. Huang, IOP SciNotes **1**, 035205 (2020).

[61] T. Rakovszky, S. Gopalakrishnan, S. A. Parameswaran, and F. Pollmann, Phys. Rev. B **100**, 125115 (2019).

[62] The spreading behaviors of EE and quasiparticles do not have to be consistent (see, e.g., Ref. [20], where the authors argued that the spreading of EE or information can be faster than that of the particles or quasiparticles). In the cases that both are ballistic, there can exist a coefficient between the velocities (and their upper bounds) of EE and quasiparticles (denoted as v and v_q, respectively), i.e., $v = \gamma v_q$ [63]. For the velocity of quasiparticles, it has been obtained that its upper bound for the quantum Ising chain in a uniform and time-independent magnetic field is $v_q^{max} = 2$ (Lieb-Robinson bound). We obtain the velocity of EE $v = 2.76$ under VEEF in the $N = 10$ quantum Ising chain with periodic boundary condition, which is larger than 2. This implies the velocity of EE spreading can be faster than that of the quasiparticles under VEEF, possibly because the VEEF is optimized to enhance the EE while being time dependent and spatially inhomogeneous.

[63] J. Schachenmayer, B. P. Lanyon, C. F. Roos, and A. J. Daley, Phys. Rev. X **3**, 031015 (2013).

[64] T. c. v. Prosen, Phys. Rev. E **65**, 036208 (2002).

[65] L. Zhang, H. Kim, and D. A. Huse, Phys. Rev. E **91**, 062128 (2015).

[66] L. Zhang, V. Khemani, and D. A. Huse, Phys. Rev. B **94**, 224202 (2016).

[67] M. Akila, D. Waltner, B. Gutkin, and T. Guhr, J. Phys. A **49**, 375101 (2016).